Structural Studies of Detergent-Solubilized and Vesicle-Reconstituted Low-Density Lipoprotein (LDL) Receptor†

Kumkum Saxena‡ and G. Graham Shipley*

Departments of Biophysics and Biochemistry, Center for Advanced Biomedical Research, Boston University School of Medicine, Boston, Massachusetts 02118

Received June 30, 1997; Revised Manuscript Received October 20, 1997⊗

ABSTRACT: The low-density lipoprotein (LDL) receptor plays a key role in maintaining circulating and cellular cholesterol homeostasis. The LDL receptor is a transmembrane glycoprotein whose biochemical and genetic properties have been extensively studied notably by Brown, Goldstein and colleagues [Brown, M. S., & Goldstein, J. L., (1986) *Science 232*, 34−47]. However, few if any structural studies of the LDL receptor have been reported, and details of its secondary and tertiary structure are lacking. In an attempt to determine the low-resolution structure of the LDL receptor, we have purified the receptor from bovine adrenal cortices using modifications of the method of Schneider et al. [Schneider, W. J., Goldstein, J. L., & Brown, M. S. (1985) *Methods in Enzymol. 109*, 405−417]. Using circular dichroism, the secondary structure of the detergent-solubilized bovine LDL receptor at 25 °C was shown to be 19% α-helix, 42% β-sheet, and 39% random coil. Interestingly, the detergent-solubilized receptor appeared to be quite resistant to changes in secondary structure over the temperature range 10−90 °C, with only minor but reversible changes being observed. In contrast, a more pronounced unfolding of the detergent-solubilized receptor was observed in the presence of guanidinium hydrochloride. Using the complete sequence of the human LDL receptor, sequence analysis by the Chou−Fasman prediction algorithm showed quite good agreement with the experimentally determined secondary structure of the bovine LDL receptor at 25 °C. Finally, the purified, bovine LDL receptor was reconstituted into large unilamellar vesicles of egg yolk phosphatidylcholine using a procedure exploiting preformed vesicles and detergent dialysis. We showed previously using negative stain electron microscopy that reconstituted vesicles bind LDL. Now, using cryoelectron microscopy of frozen hydrated reconstituted vesicles evidence of an extended, stick-like morphology (length ∼120 Å) for the extracellular domain of the LDL receptor has been obtained. Successful purification of the receptor, its incorporation into single bilayer vesicles, and its direct visualization by cryoelectron microscopy pave the way for more detailed structural studies of the LDL receptor and the receptor−LDL complex.

The LDL[1] receptor is a cell surface glycoprotein that binds cholesterol-rich lipoproteins via their apoproteins $apoB_{100}$ and apoE and internalizes the bound lipoprotein through the process of endocytosis (Brown & Goldstein, 1986; Goldstein et al., 1985). The LDL receptor is a class II receptor that functions to deliver LDL cholesterol to cells and to remove LDL particles from the circulation (Pittman et al., 1982). The LDL receptor is found in most cell types but is most abundant in the adrenal cortex where delivered LDL cholesterol is used in the synthesis of steroid hormones (Schneider et al., 1979). The liver uses the LDL receptor pathway to clear LDL from the circulation; a steady-state level of LDL cholesterol is maintained by the LDL receptor pathway. The LDL receptor pathway can be divided into four key events: (i) binding of ligand (e.g. LDL) to the receptor located in coated pits, (ii) internalization of the LDL−LDL receptor complex through coated vesicles, (iii) recycling of the LDL receptor to the cell surface, and (iv) degradation of LDL and release of free cholesterol. The released LDL cholesterol inhibits both intracellular production of cholesterol through regulation of HMGCoA reductase and synthesis of new LDL receptor via gene regulation (Yokoyama et al., 1993).

The LDL receptor is synthesized as a 120 kDa precursor which is converted into a mature receptor of apparent molecular mass 160 kDa following post-translational modification in the Golgi apparatus (Cummings et al., 1983). The primary structure of the LDL receptor from several different species has been determined [see, for example, Schneider (1989)]. The human LDL receptor contains 860 residues, including a 21 aa N-terminal signal sequence that is removed co-translationally (Yamamoto et al., 1984). On the basis of the primary sequence, the LDL receptor can be divided into five domains (Esser et al., 1988): I, the apoB and apoE ligand-binding domain (292 aa) containing seven imperfect copies of a 40 aa cysteine-rich sequence; II, the EGF precursor homology domain (400 aa) perhaps involved in LDL release in endosomes; III, the O-linked sugar domain

† This research was supported by Research Grants HL-26335 and HL-57405, and by Training Grant HL-07291 from the National Institutes of Health.

* To whom correspondence should be addressed.

‡ Present address: Department of Medicine, Brigham and Women's Hospital and Harvard Medical School, Boston, MA 02115.

⊗ Abstract published in *Advance ACS Abstracts,* December 1, 1997.

[1] Abbreviations: LDL, low-density lipoprotein; aa, amino acid; PMSF, phenylmethylsulfonyl fluoride; GnDHCl, guanidinium hydrochloride; β-OG, β-octyl glucopyranoside; CD, circular dichroism; MLV, multilamellar vesicles; LUV, large unilamellar vesicles; SDS−PAGE, sodium dodecyl sulfate−polyacrylamide gel electrophoresis; EYPC, egg yolk phosphatidylcholine; ECL, enhanced chemiluminescence; BSA, bovine serum albumin; HRP, horseradish peroxidase.

S0006-2960(97)01579-1 CCC: $14.00

(58 aa) of unknown function; IV, the membrane spanning domain (22 aa); and V, the cytoplasmic domain (50 aa) containing the N-P-X-Y clustering signal that is involved in the clustering of the LDL receptor in coated pits.

Several mutations that impair the LDL receptor have been identified and grouped into five classes (Soutar, 1992). They include mutants that produce (i) no LDL receptor, (ii) LDL receptor that is not transported to the plasma membrane, (iii) LDL receptor incapable of binding LDL, (iv) LDL receptor that fails to cluster in coated pits, and (v) LDL receptor that does not dissociate from its bound ligand and does not recycle. Such genetic defects in the LDL receptor decrease hepatic clearance of LDL, resulting in elevated levels of circulating LDL (and cholesterol) (Goldstein & Brown, 1982). This defect, familial hypercholesterolemia, ultimately leads to cholesterol accummulation in other tissues and is directly related to the process of atherosclerosis [Goldstein & Brown, 1983).

Although the biochemistry, cell biology, and genetics of the LDL receptor have been worked out in great detail by Brown, Goldstein, and their colleagues (Goldstein et al., 1985; Brown & Goldstein, 1986), surprisingly few structural or biophysical studies have been performed on this important receptor. Sequence analysis and secondary structure predictions have been reported (De Loof et al., 1986). Recently, Kroon, Smith, and colleagues have expressed the N-terminal cysteine-rich repeat (LB1) of the ligand-binding domain of the LDL receptor and characterized its intradomain disulfide linkage scheme (Bieri et al., 1995). Furthermore, these investigators have shown using two-dimensional NMR methods that both this cysteine-rich repeat (LB1) and its neighbor LB2 exhibit a β-hairpin/β-turns structure, although structural and dynamic differences do exist between the two subdomains (Daly et al., 1995a,b).

Our own studies have focused on (i) purifying the LDL receptor from bovine adrenal cortex, (ii) studying the detergent-solubilized LDL receptor by structural and spectroscopic methods, (iii) reconstituting the LDL receptor into lipid vesicles, (iv) studying reconstituted LDL receptor by structural methods, and (v) developing oriented membrane systems containing LDL receptor to which its ligand LDL can be bound in an orientationally restricted way (Saxena & Shipley, 1992; Saxena, 1994). Our initial goal is to provide a low-resolution picture of LDL receptor with its major extracellular domains mapped by ligand or antibody labeling; a longer term goal will be to produce higher resolution structural descriptions of the LDL receptor itself and its bound ligand LDL.

MATERIALS AND METHODS

The hybridoma line secreting monoclonal antibody IgG-C7 (Beisiegel et al., 1981) was obtained from the American Type Culture Collection (Rockville, MD). IgG-C7 was purified from the mouse ascites. Monoclonal antibody IgG-4A4 was kindly provided by Drs. M. S. Brown and J. L. Goldstein (University of Texas Southwestern Medical Center, Dallas, Texas). Rabbit anti-mouse IgG (Calbiochem, La Jolla, CA) and was labeled with ^{125}I using enzymobeads (Bio-Rad Laboratories, Hercules, CA). Human LDL ($d = 1.025-1.050$ g/mL) was obtained from the plasma of individual healthy subjects and prepared by ultracentrifugation as previously described (Lindgren et al., 1972). Affinity columns were prepared by cross-linking IgG-C7 and LDL to CNBr-Sepharose (Pharmacia Biotech Inc., Piscataway, NJ) according to the manufacturer's instructions.

Isolation and Purification of the Bovine LDL Receptor

Procedures for isolating and purifying the LDL receptor have been established by Schneider et al. (1980, 1982, 1985). Cortices from 30−50 bovine adrenal glands were homogenized at 4 °C in Buffer A (50 mM Tris-chloride, pH 8.0, 0.15 M NaCl, 1 mM PMSF, and 0.1 mM leupeptin), centrifuged at 800*g* for 10 min and the supernatant was filtered through Miracloth. The filtrate was centrifuged at 100000*g* for 1 h. The membrane pellet was resuspended in Buffer B (250 mM Tris-maleate, pH 6.0, 2 mM $CaCl_2$, 1 mM PMSF, and 0.1 mM leupeptin) and sonicated briefly. The membrane suspension was adjusted to 154 mM NaCl, solubilized with 1% Triton X-100, and centrifuged at 100000*g* for 1 h (4 °C) to remove unsolubilized material. The supernatant was diluted into a 3-fold excess of Buffer C (10 mM Tris-maleate, pH 6.0, 2 mM $CaCl_2$, 1% Triton X-100, 1 mM PMSF, 0.05 mM leupeptin) to lower the ionic strength. The Triton X-100 extract was applied to a 2.6 × 8 cm DEAE-cellulose (DE-52, Whatman) column preequilibrated with Buffer D (50 mM Tris-maleate, pH 6.0, 2 mM $CaCl_2$, 1% Triton X-100, 1 mM PMSF and 0.05 mM leupeptin) at a rate of 70 mL/h. The column was washed with Buffer D followed by Buffer E (50 mM Tris-maleate, pH 6.0, 2 mM $CaCl_2$, 40 mM β-octylglucopyranoside (β-OG), 1 mM PMSF, and 0.01 mM leupeptin). The receptor was eluted with a linear gradient of 120 mL of NaCl (0−250 mM NaCl) in Buffer E. Fractions of 5 mL were collected, and a dot blot assay was performed on the ion-exchange fractions: 100-μL aliquots of the ion-exchange fractions were applied to nitrocellulose paper (Schleicher and Schuell, Keene, NH) using a Bio-Rad dot blot apparatus. The wells were washed with 100 μL of Buffer E. The paper was removed from the apparatus and incubated for 1 h at room temperature in 20 mM Tris-HCl, pH 7.6, 137 mM NaCl, 0.1% Tween (Buffer G) containing 5% non-fat dry milk followed by incubation for 2 h at room temperature in Buffer G containing 1:2000× diluted IgG-C7 ascites. The paper was then washed three times (15 min each) with 100 mL of Buffer G. The washed nitrocellulose paper was incubated with 1:10 000× diluted horseradish peroxidase (HRP) labelled anti-mouse rabbit antibody (Calbiochem, La Jolla, CA). The paper was again washed as described above and then treated for 1 min with Amersham (Arlington Heights, IL) enhanced chemiluminiscence reagent, followed by exposure of the paper to Kodak XAR-5 film. The peak fractions from the ion-exchange column containing LDL receptor were pooled and diluted with 3 vol of Buffer F (50 mM Tris-chloride, pH 8.0, 2 mM $CaCl_2$, 50 mM NaCl, 1 mM PMSF, 0.05 mM leupeptin). The diluted DEAE-cellulose fraction was centrifuged at 100000*g* to clarify the solution. The supernatant was applied to either an LDL-Sepharose or an IgG-C7-Sepharose column previously equilibrated with Buffer F. The column was washed with 500 mL of Buffer F followed by 3 vol of water, and the purified receptor was eluted from the column with a 0.5 M solution of NH_4OH. The eluate containing the LDL receptor was fractionated into aliquots and quickly frozen in liquid nitrogen. The frozen receptor was lyophilized and stored at −70 °C. Purified receptor was analyzed using 7% SDS−

polyacrylamide gel electrophoresis under non-reducing conditions as described by Laemmli (1970). LDL receptor was detected by immunoblot analysis using IgG-C7 and IgG-4A4 as primary antibodies and ^{125}I-labeled rabbit anti-mouse IgG as secondary antibody as described by Beisiegel et al. (1982).

For the LDL-binding assay, increasing amounts (3, 6, 12, 24, and 30 ng) of the affinity-purified receptor (in duplicates) in Buffer H (50 mM Tris-maleate, pH 6.0, 2 mM $CaCl_2$, 50 mM NaCl) were blotted onto nitrocellulose paper using the Bio-Rad dot blot apparatus. The wells were washed with Buffer H. The nitrocellulose paper was then blocked with 5% BSA in Buffer I (50 mM Tris-HCl, pH 8.0, 50 mM NaCl, 0.5% BSA) for 1 hour at room temperature. This was followed by incubation with LDL (45 μg/mL) in Buffer I containing 2 mM $CaCl_2$ either in the absence (Set 1) or presence (Set 2) of 10 mM EDTA and 2 mM EGTA (see Figure 2). The blot was washed twice with Buffer I for 15 min, followed by incubation in Buffer I containing 1:8000× diluted HRP-labeled polyclonal anti-human apoB antibody (Biodesign International, Kennebunk, ME). The blot was washed as described above and bound antibody visualized by chemiluminiscence and exposure to Kodak XAR-5 film.

Secondary Structure Prediction

The Chou−Fasman algorithm for predicting secondary structure based on 64 protein structures (Chou & Fasman, 1974a,b) was kindly provided by Dr. Fasman (Brandeis University, Waltham, MA). This program was used to estimate the overall secondary structure of the human LDL receptor. Human LDL receptor shares an 80% sequence homology with the the sequenced C-terminal fragment (264 aa) of bovine LDL receptor. In the absence of a complete sequence of bovine LDL receptor, the secondary structure predictions were made on the putative five domains (see above) of the *human* LDL receptor. The overall distribution of α-helix, β-sheet, and β-turns in the entire protein has also been predicted.

Circular Dichroism

CD spectra were obtained over the range of approximately 180−250 nm using an AVIV 62DS CD spectrophotometer (AVIV Associates, Inc., Lakewood, NJ) with a thermoelectric temperature controller allowing temperature control to ±0.1 °C. The instrument was calibrated from 500 to 190 nm with *d*-10-camphorsulfonic acid (1 mg/mL in ethanol). Temperature studies were performed in two ways: (1) by recording full spectra at specified temperatures and (2) by continuous heating at a controlled rate (3−5 s/wavelength/temperature step) from 10 to 90 °C at heating rates of 0.5−1 °C/min (wavelengths, 250 nm, "baseline", zero change; 208 or 222 nm α-helix; 217 nm, β-sheet). Most measurements were made by using 0.2 and 0.5 mm pathlength cells and LDL receptor solutions (in 200−300 mM β-OG) of approximately 300−600 μg/mL. Unless otherwise specified, all spectra were recorded at 25 °C with a 0.5 s time constant. For temperature studies, 0.5 mm path length cells and LDL receptor concentrations of approximately 200 μg/mL were used. For denaturation studies using guanidinium hydrochloride (GnDHCl), LDL receptor was dialyzed in HEPES buffer (5 mM HEPES, 5 mM β-OG, pH 7.0, 2 mM $CaCl_2$). LDL receptor in HEPES buffer was incubated with 7.5 M GnDHCl in HEPES buffer so that the final concentration of LDL receptor was around 100 μg/mL and the GnDHCl concentration was 0, 1, 2, 3, 4, and 6 M. Samples were incubated overnight at 4 °C before the CD spectra were recorded. Protein concentrations were determined using Micro BCA Protein Assay Reagent Kit (Pierce, Rockford, IL). The program PROSEC (Chang et al., 1978) was used to estimate the overall secondary structure of the receptor.

Reconstitution of the LDL Receptor and Electron Microscopy

Large unilamellar vesicles of egg yolk phosphatidylcholine (EYPC) were prepared by the extrusion technique (Madden & Cullis, 1984) using a Lipex Extruder (Lipex Co., Vancouver, Canada). The detergent-solubilized LDL receptor was added to the the preformed vesicles and the detergent removed by dialysis. The whole procedure was performed at room temperature. EYPC, 10 mg (Lipid Products, Nutfield, U.K.), in ethanol was placed in a 50 mL round bottom flask and dried by rotary evaporation. The thin film of EYPC was brought into solution with 1 mL of ether. The lipid was dried again by rotary evaporation, and the whole process repeated. The lipid was further dried by overnight lyophilization. The dry thin film of EYPC was then hydrated with 1 mL of HEPES buffer (10 mM HEPES, pH 7.0, 2 mM $CaCl_2$). To ensure adequate hydration of the lipid, a freeze−thaw protocol was followed. The lipid sample was placed in a cryotube and frozen in liquid nitrogen for approximately 30 s. The cryotube was then removed from liquid nitrogen and plunged into warm water (40−60 °C). When the sample thawed, the cycle was repeated five times. At this stage, multilamellar vesicles (MLVs) were formed. The frozen and thawed MLVs were then passed through 0.1 μm pore size polycarbonate filters (Nucleopore 110605) by extrusion. To produce large unilamellar vesicles (LUV) of about 1000 Å in diameter, the lipid sample was passed through the filter a minimum of 10 times. LUVs (100 μL, 10 mg/mL) were mixed with 100 μL of LDL receptor (2 mg/mL) in 400 mM β-OG to give a final concentration of 5 mg/mL (6.25 mM) EYPC, 1 mg/mL (6.25 μM) LDL receptor, and 200 mM β-OG. The dialysis step was performed at room temperature against three changes of 6 L of buffer for a total of 48 h. Control EYPC vesicles were prepared by similar methods except that protein-free buffer solutions replaced the LDL receptor solutions.

Frozen hydrated specimens for cryoelectron microscopy were prepared by rapidly plunging thin films of LDL receptor/EYPC vesicles or vesicles containing no receptor, into liquid ethane cooled to just above its freezing point. A 6 μL sample was applied to 400-mesh copper grids covered with holey carbon films. Most of the sample was blotted away with filter paper, leaving films of solution over many of the holes, and the grids were dropped into nearly solidified ethane cooled with liquid nitrogen. The grids were transferred to and stored under liquid nitrogen until use. Grids containing frozen samples were loaded under liquid nitrogen into a Gatan cold stage. Images were recorded with a Philips CM12 electron microscope at a magnification of 75 000 to 100 000× under low dose conditions, and at a defocus of −1.0 μm on Kodak SO163 film. The low dose negatives

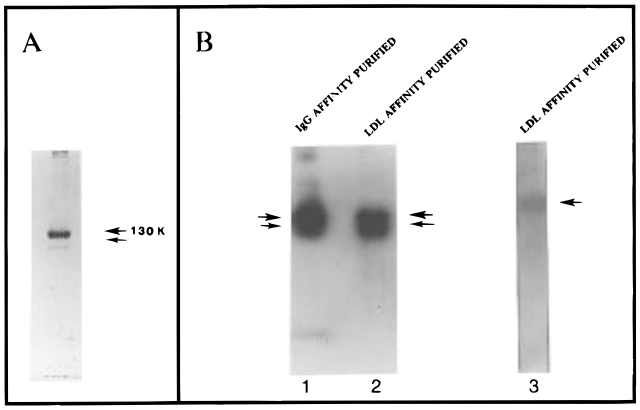

FIGURE 1: Affinity chromatography of the LDL receptor. (A) SDS−polyacrylamide gel electrophoresis under reducing conditions. The gel was stained with Coomassie Blue. (B) Immunoblot analysis of the immunoaffinity and the LDL−affinity purified receptor. Lanes 1 and 2, IgG-C7− and LDL−affinity purified receptor, respectively, detected with IgG-C7 and a secondary antibody labeled with ^{125}I. Lane 3, LDL-affinity purified receptor detected with IgG-4A4 and ^{125}I-labeled secondary antibody.

were developed in full-strength Kodak developer D19 for 12 min.

RESULTS

Purification and Characterization of the Bovine LDL Receptor

LDL receptor was purified to homogeneity from bovine adrenal glands following the methods of Schneider et al. (1985). About 600 μg of purified receptor was obtained from about 50 adrenal glands. Figure 1A shows the SDS−PAGE of the LDL receptor purified by affinity chromatography on monoclonal IgG-C7-Sepharose. The affinity purified receptor is very homogeneous and migrates at 130 kDa under non-reducing conditions. A minor band that is observed in most of the preparations has an apparent molecular mass of 108 kDa. The receptor purified using an LDL affinity column also contains this minor contaminant (data not shown). The nature of the minor contaminant observed in the affinity-purified LDL receptor preparations was investigated by immunoblot analysis using monoclonal antibodies IgG-C7 and IgG-4A4 (antibodies against the N-terminus and the C-terminus region of the LDL receptor, respectively). Figure 1B shows the immunoblots of the LDL receptor purified by immunoaffinity and LDL-affinity chromatography. Lane 1 represents the immunoaffinity purified LDL receptor treated with the N-terminus monoclonal antibody IgG-C7 and a secondary antibody labeled with ^{125}I. This antibody, as expected, recognizes both the major and the minor bands seen on SDS−PAGE of affinity-purified receptor (Figure 1A). The LDL affinity-purified receptor also shows two bands on the immunoblot when the N-terminus antibody, IgG-C7, was used as the primary antibody (lane 2). On the other hand, when the C-terminus antibody, IgG-4A4, was used (lane 3), only the major band (130 kDa) showed up on the immunoblot. Therefore, the minor band on the SDS−PAGE of the purified receptor probably represents a degradation product that lacks the C-terminal end of the receptor. It should be emphasized that the Coomassie Blue-stained SDS−PAGE shown in Figure 1A provides a more accurate representation of the relative amounts of the 130 and 108 kDa bands than Figure 1B. The Western blot that has been overexposed to emphasize that the 108 kDa contaminant was recognized by IgG-C7 (Figure 1B, lanes 1 and 2) and not IgG-4A4 (Figure 1B, lane 3). Clearly, the band at 108 kDa (Figure 1A) represents a very minor contaminant.

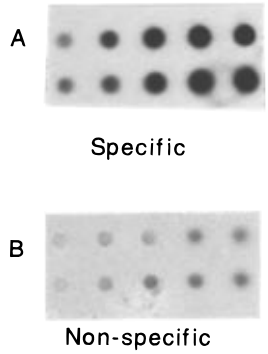

FIGURE 2: LDL-binding assay of affinity-purified LDL receptor using the ECL system. Increasing amounts of the purifed receptor in duplicate were blotted onto nitrocellulose paper. The blot was treated with LDL in the presence (A) and absence (B) of calcium, followed by a polyclonal antibody against LDL. Finally, the blots were treated with a secondary antibody labeled with horseradish peroxidase and detected using the ECL system.

Figure 2 shows the LDL-binding assay using the ECL system. From left to right, increasing amounts of the affinity-purified receptor were blotted onto nitrocellulose paper. Set 1 represents the specific binding of LDL to the receptor in the presence of calcium, whereas Set 2 represents the nonspecific binding of LDL in the absence of calcium. The binding of LDL to the receptor is insignificant in the absence of calcium ions (Set 2). In the presence of calcium (Set 1), the binding of LDL to the receptor is significantly enhanced with an approximately linear dependence in the lower concentration range.

Secondary Structure Prediction

Using the Chou−Fasman algorithm, the overall secondary structure of the human LDL receptor has been predicted; 22.6% of the protein has been assigned α-helix, and the predicted β-sheet for the receptor is 24.5%. A large percentage (38.6%) of the protein is predicted to be β-turns. The distribution of α-helix, β-sheet, and β-turns in each of the five domains of the LDL receptor has also been predicted and is presented in Table 1.

Domain I: Ligand Binding Domain (1−292 aa). The average α-helical ($\langle P_\alpha \rangle$), β-sheet ($\langle P_\beta \rangle$), and β-turn ($\langle P_t \rangle$) potential of tetrapeptides i to $i+3$, on the basis of single-residue information and the β-turn probability profile for the ligand binding domain of the human LDL receptor, is shown in Figure 3A. The secondary structure prediction of this domain is: 14.7% α-helix, 18.5% β-sheet, and 48% β-turn (Table 1). This domain contains seven cysteine-rich imperfect repeats. The distribution of α-helix and β-sheet in these repeats is shown in Figure 4. For example, Repeats 2, 3, and 4 are predicted to contain no α-helical regions but are expected to be relatively rich in β-sheet (34.1%, 25.6%, and 26.8%, respectively). All seven repeats are predicted to contain several β-turns (Figure 4).

Domain II: EGF Precursor Homology Domain (293−692 aa). The β-turn probability and $\langle P_\alpha \rangle$, $\langle P_\beta \rangle$, and $\langle P_t \rangle$ for this domain are shown in Figure 3B. The secondary structure prediction for this domain is 26.2% α-helix, 25.2% β-sheet,

Table 1

	domain	% α-helix	% β-sheet	% β-turns	% others
I.	ligand-binding domain (1−292 aa)	14.7	18.5	48.0	18.8
II.	EGF precursor homology domain (293−692 aa)	26.2	25.2	36.0	12.5
III.	O-linked sugar domain (693−750 aa)	26.3	49.1	19.2	5.2
IV.	membrane-spanning domain (768−789 aa)	0.0	95.5	4.5	0.0
V.	cytoplasmic domain (790−839 aa)	44.0	0.0	38.0	18.0

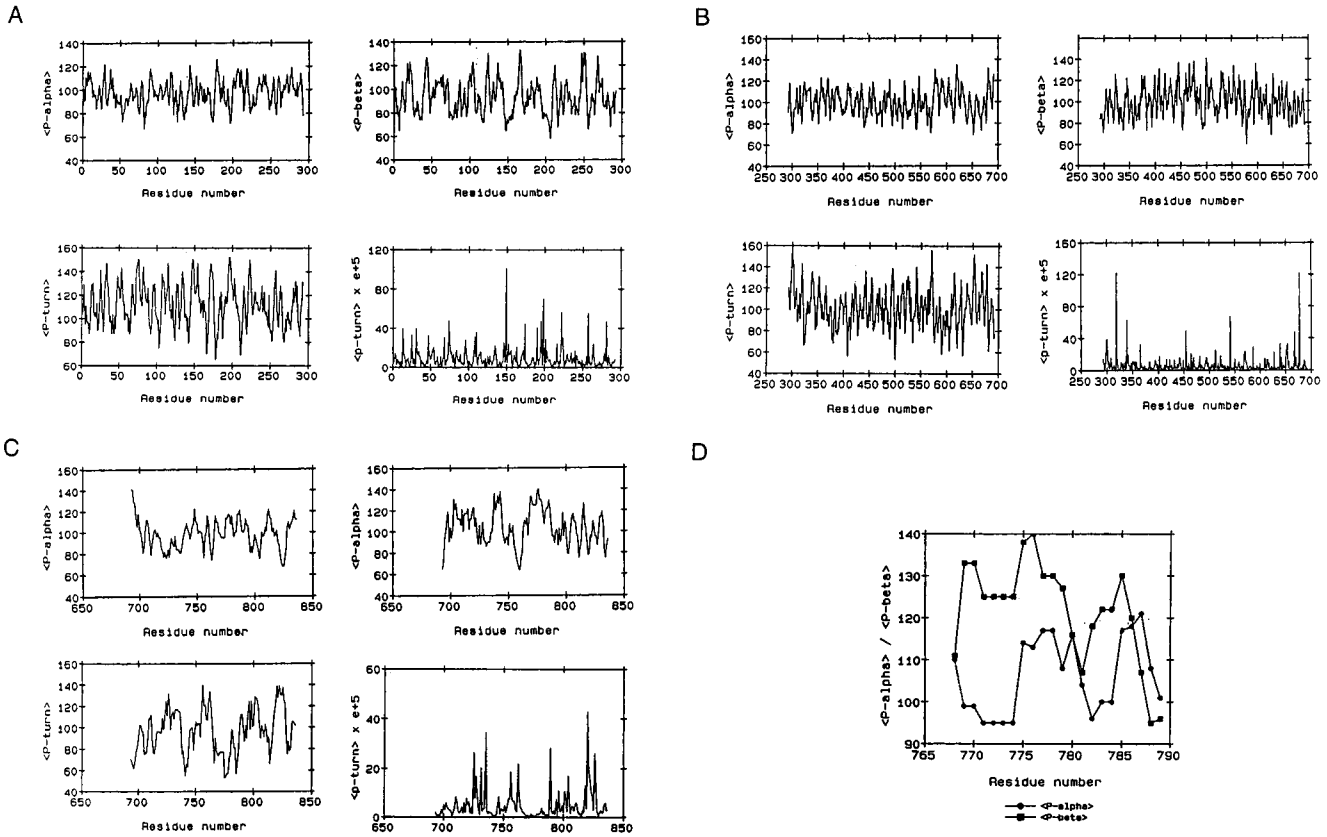

FIGURE 3: Secondary structure predictions of the five major domains of the human LDL receptor using the Chou−Fasman algorithm (1974a,b). The average α-helical, β-sheet, β-turn potential, and the β-turn probability of (A) the ligand-binding domain (residues 1−292), (B) the EGF precursor homology domain (residues 293−692), and (C) the O-linked sugar, membrane-spanning, and cytoplasmic domains (residues 693−839). (D) The average α-helical and β-sheet potential of the membrane-spanning domain (residues 768−789).

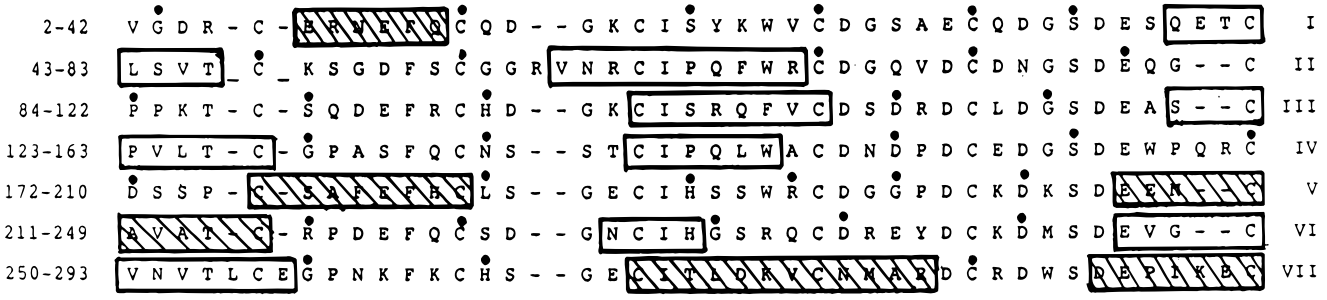

FIGURE 4: Predicted α-helical (shaded boxes), β-sheet (empty boxes), and β-turn (filled circles) regions of the seven repeats of the ligand-binding domain of the human LDL receptor based on the Chou−Fasman algorithm.

and 36% β-turn (Table 1). This is the largest domain of the receptor and has a very high percentage of predicted β-turns.

Domains III, IV, and V: O-Linked Sugar (693−750 aa), Membrane-Spanning (768−789 aa), and Cytoplasmic (790−839 aa) Domains. Figure 3C shows the $\langle P_\alpha \rangle$, $\langle P_\beta \rangle$, $\langle P_t \rangle$, and $\langle p_t \rangle$ for the three domains at the C-terminal end. The predicted values for α-helix, β-sheet, and β-turn for these three domains are given in Table 1. Interestingly, the membrane-spanning region is predicted to be 95.5% β-sheet and 4.5% β-turn. The $\langle P_\alpha \rangle$ and $\langle P_\beta \rangle$ for the membrane region is shown in Figure 3D. Almost the entire membrane-spanning region has a higher β-sheet potential than α-helix potential, although the potential for α-helix is also high. Additionally, the probability of β-turns in this region is very low.

On the other hand, the cytoplasmic (50 aa) domain is predicted to be almost entirely α-helical and β-turns. The proposed internalization signal of the cytoplasmic tail of the LDL receptor (NPVY) is predicted to form a β-turn. This is in accordance with the NMR studies of Bansal

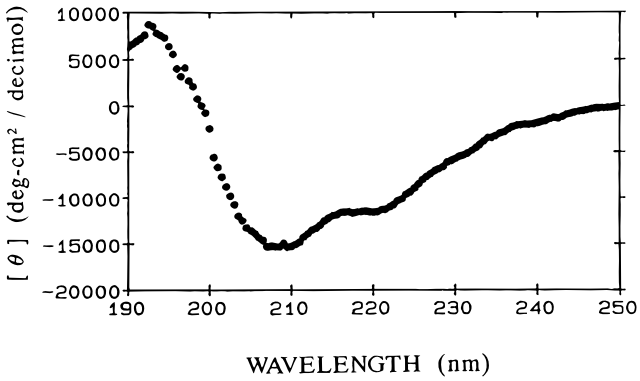

FIGURE 5: Far-UV circular dichroism spectrum of the detergent-solubilized bovine LDL receptor at 25 °C.

and Gierasch (1991) who have shown that the NPVY sequence of the the cytoplasmic domain adopts a reverse turn conformation.

Circular Dichroism of Purified Bovine LDL Receptor

Circular dichroism was used to determine the overall secondary structure of detergent-solubilized LDL receptor. Figure 5 shows the far-UV CD spectrum of the receptor in 200 mM β-OG. Two minima are observed at 208 and 222 nm as well as a maximum at around 193 nm. On the basis of analysis using the PROSEC algorithm (Chang et al., 1978), detergent-solubilized LDL receptor contains 19% α-helix, 42% β-sheet, and 39% random coil.

The unfolding of bovine LDL receptor in the detergent-solubilized form was studied as a function of temperature and concentration of the denaturant, guanidinium HCl (GnDHCl). The effect of temperature (10−90 °C) on detergent-solubilized bovine LDL receptor (in 5 mM HEPES, 5 mM β-OG, and 2 mM $CaCl_2$, pH 7.0) was studied by recording the molar ellipticity at (a) 208 and 222 nm (changes in the α-helix content) and (b) 217 nm (changes in the β-sheet content). As a control, the molar ellipticity at 250 nm was also recorded as a function of temperature. Figure 6B shows the unfolding of bovine LDL receptor (in detergent) as a function of temperature. Relatively small changes in the secondary structure of the LDL receptor as a function of temperature were observed with no marked discontinuity as would be seen in a cooperative melting process. No significant change is observed in the theta values at 217 and 222 nm as a function of temperature, whereas a small but noticeable decrease in molar ellipticity with increasing temperature is seen at 208 nm. This is more apparent in Figure 6A which shows a comparison of the CD spectra recorded at 25 and 90 °C. The two spectra are very similar in the wavelength region 215−227 nm and below 197 nm but differ over the range 197−215 nm. On a qualitative basis a lower value of molar ellipticity at 208 nm indicates lower α-helix content at 90 °C compared to that at 25 °C. The CD spectra recorded at 25 °C before (Figure 6A) and after (data not shown) the melting studies are identical, suggesting that the minor changes observed are indeed reversible. The presence of the detergent β-OG presumably plays a role in preventing complete unfolding of the receptor with temperature.

The unfolding of detergent-solubilized LDL receptor was also studied as a function of GnDHCl concentration. Figure 7A shows the far-UV CD spectra of the receptor at 25 °C at various GnDHCl concentrations. At high GnDHCl concentrations, the data below 210 nm were not very reliable due to large scattering effects. At 0 M GnDHCl concentration, the protein is in its folded conformation, albeit in the presence of detergent. The fraction unfolded as recorded at 224 nm was calculated for all concentrations of GnDHCl used. The plot of fraction unfolded as a function of GnDHCl concentration is shown in Figure 7B. The LDL receptor unfolds as the GnDHCl concentration increases, and finally around 3 M GnDHCl it unfolds almost to its maximum. The midpoint of the unfolding curve is somewhere between 1

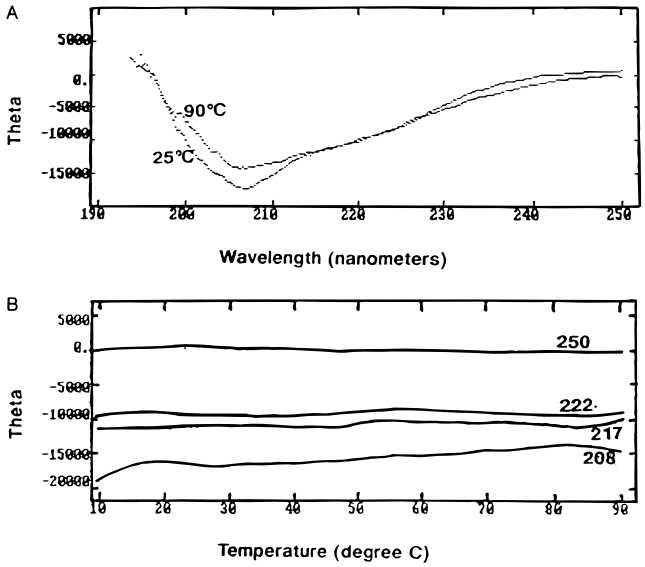

FIGURE 6: (A) Comparison of the far-UV circular dichroism spectrum of the detergent-solubilized bovine LDL receptor at 25 and 90 °C. (B) Unfolding of the detergent-solubilized bovine LDL receptor as a function of temperature. Plot of molar ellipticity as a function of temperature at wavelengths 208, 217, 222, and 250 nm.

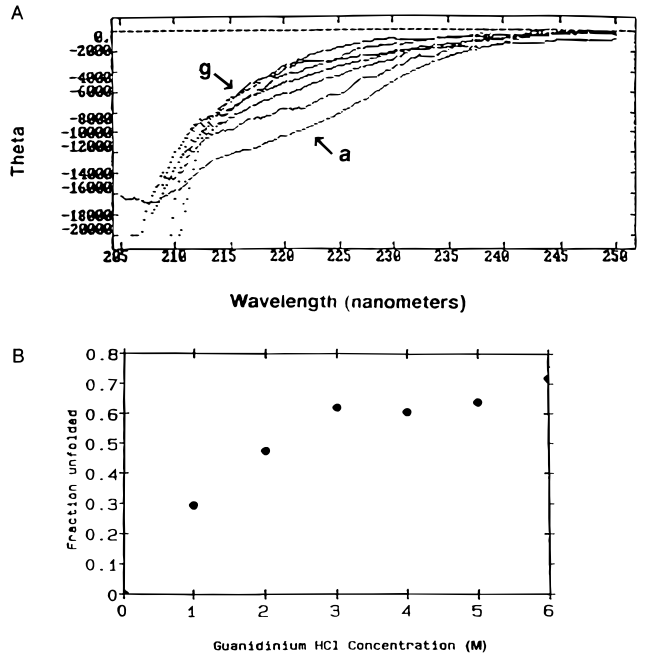

FIGURE 7: (A) Comparison of the far-UV circular dichroism spectrum of the detergent-solubilized bovine LDL receptor as a function of guanidinium-HCl concentration (a, 0 M; b, 1 M; c, 2 M; d, 3 M; e, 4 M; f, 5 M; g, 6 M). (B) Fraction of unfolded LDL receptor as a function of guanidinium-HCl concentration as determined by the molar ellipticity at 224 nm.

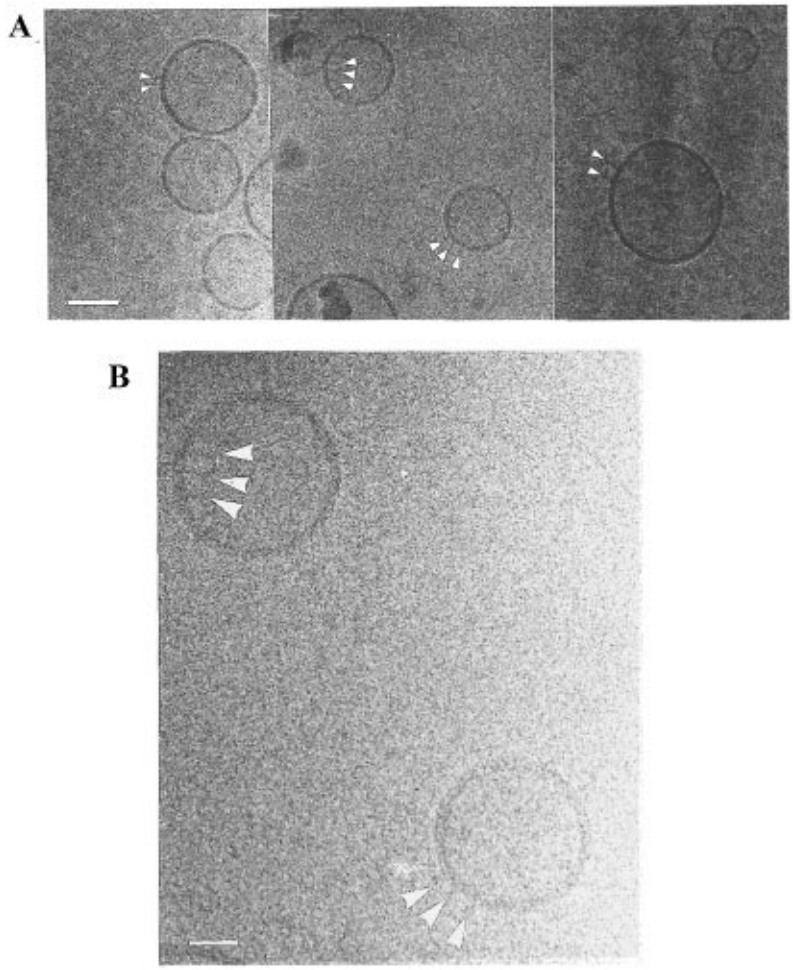

FIGURE 8: Cryoelectron microscopy of EYPC vesicle-reconstituted bovine LDL receptor: (A) magnification, 187 500× (bar = 50 nm); (B) magnification, 450 000× (bar = 20 nm).

and 2 M GnDHCl. Complete unfolding of the receptor does not occur even at 6 M GnDHCl.

Reconstitution of the LDL Receptor and Cryoelectron Microscopy

LDL receptor−EYPC vesicles were prepared by the solubilization of preformed vesicles followed by detergent dialysis. The protein to lipid ratio was kept at a weight ratio 1:5 (1:1000 molar). Typical electron micrographs (defocus, 1 μm; magnification, 187 500×) of large vesicles containing the LDL receptor are shown in Figure 8A. Unilamellar vesicles differing in size (mainly diameter 2000−3000 Å) were obtained, most of the vesicles being intact and spherical in shape. Arrows in Figure 8A indicate the location of linear LDL receptor particles extending from either the external or internal surfaces of the vesicle bilayer. No such particles are observed in EYPC vesicles not containing the LDL receptor (data not shown). At higher magnification (450 000×, Figure 8B) LDL receptor molecules with a stick-like or Y-shaped morphology are observed. The linear dimension of the extramembrane domain is in the range 110−130 Å.

DISCUSSION

Purification of the LDL Receptor

The LDL receptor has been purified from bovine adrenal glands using a modified version of the method developed by Schneider et al. (1985). The purification scale has now been upgraded to 30−50 adrenal glands and 500−600 μg of receptor is routinely purified in one preparation. Under non-reducing conditions, SDS−PAGE of affinity-purified receptor showed a dominant band at 130 kDa and a minor band at 108 kDa. The monoclonal antibody IgG-C7 against the N-terminal end of the receptor recognizes both the major and minor bands. However, IgG-4A4, the monoclonal antibody against the C-terminal end of the receptor, recognizes only the major band, suggesting the absence of the C-terminal domain in the minor band. Tollenshaug et al. (1982) have shown that in human fibroblasts, the LDL receptor is synthesized as a precursor of apparent molecular mass 120 kDa, which is converted to a mature form of apparent molecular mass 160 kDa as determined by SDS−PAGE under reducing conditions. However, the possibility that the weak minor band corresponds to the precursor form of the receptor appears to be ruled out because it was not recognized by the C-terminal antibody. Rather, in this case the minor band most likely represents a degradation product of the mature receptor that retains the ability to bind both the N-terminal antibody and LDL, the *in vivo* ligand of the receptor. The cytoplasmic C-terminal domain of the LDL receptor contains only 50 amino acid residues, and the transmembrane domain is composed of 20 amino acid residues (Yamamoto et al., 1984). The difference in molecular weight of the mature receptor (130 kDa, major band) and its degradation product (108 kDa, minor band) suggests that the cleavage site lies in the extracellular domain close

to the membrane surface. Thus, the 108 kDa band probably represents LDL receptor lacking both the cytoplasmic and transmembrane domains. As such, this shortened receptor lacking the hydrophobic transmembrane domain could be considered a useful candidate for crystallization studies provided it can be purified in sufficiently large amounts.

Secondary Structure

Lacking extensive information on the secondary and tertiary structures of membrane proteins in general and lipoprotein receptors in particular, we have used the predictive methods developed by Chou and Fasman (1974a,b) to derive secondary structure information for the LDL receptor. For this we used the amino acid sequence derived from the sequence of a full-length cloned 5.3 kb cDNA for the human LDL receptor (Yamamoto et al., 1984). For the human LDL receptor we obtain overall values of 23% α-helix, 25% *β*-sheet, and 39% *β*-turns. This distribution of secondary structure is in reasonable agreement with that reported previously by De Loof et al. (1986) using a similar algorithm (20% α-helix, 30% *β*-sheet, and 30% *β*-turns) and with the CD-derived distribution for the bovine receptor (19% α-helix, 42% *β*-sheet, and 39% random coil).

The amino acid sequence deduced from the cDNA sequence suggests five domains in the 839 amino acid protein. For the ligand-binding region (Domain I) the overall secondary structure is predicted by the Chou−Fasman algorithm to be 15−20% α-helix and *β*-sheet, together with a high level (approximately 50%) of *β*-turns (Figures 3A and 4; Table 1). In good agreement with these predictions, recent NMR studies of the first and second cysteine-rich repeats indicate a high level of *β*-turn and *β*-hairpin structures particularly toward the C-terminal end of these approximately 40-residue sequences (Daly et al., 1995a,b). The EGF-precursor homology (Domain II) and O-linked sugar (Domain III) regions show increases in α-helix and *β*-sheet content, with lower levels of *β*-turn. The cytoplasmic domain (Domain V) is predicted to be rich in α-helix (44%) and *β*-turn, with no *β*-sheet being indicated.

While the Chou−Fasman algorithm based on the crystal structures of globular, nonmembrane proteins is clearly appropriate for the extramembrane domains of the LDL receptor (Domains I, II, III, and V), it is perhaps less appropriate for the membrane-spanning Domain IV. While the Chou−Fasman algorithm suggests a predominantly *β*-sheet structure for the short, 22-residue transmembrane domain (Domain IV), a high potential for α-helix structure is also predicted (see Figure 3). Because a single 22-residue transmembrane *β*-strand is energetically unfavorable, it is likely that the transmembrane region takes the form of an α-helix. A possible reason for predicting a *β*-strand conformation for this domain has been suggested by Jahnig (1989) indicating that the most hydrophobic residues, which are associated with *β*-strand conformations in water-soluble proteins, are also found in α-helix structures of membrane proteins [also, see Fariselli et al. (1993)].

Circular Dichroism

Far-UV CD spectroscopy has been used to study the folding and unfolding of protein secondary structure either at equilibrium or kinetically. The thermal studies of detergent-solubilized LDL receptor by CD (Figure 6) show that the receptor is resistant to change in overall secondary structure with temperature. This could be partly due to a detergent effect whereby the secondary structure of the receptor is stabilized by the detergent. In addition, the N-terminal domain (Domain 1) accounting for 35% of the receptor is probably resistant to unfolding due to its stabilization by the multiple disulfide bonds present within each of the seven cysteine-rich repeats. The minor changes observed in secondary structure are reversible, demonstrating that the receptor folds back into its original conformation when cooled back to 25 °C. Interestingly, GnDHCl appears to have a more pronounced effect than temperature on the secondary structure of the receptor (see Figures 6 and 7). On the basis of data at 224 nm, unfolding of approximately 70% of the LDL receptor occurs at 6 M GnDHCl with a midpoint of unfolding at approximately 1.5 M GnDHCl.

Reconstitution of the LDL Receptor and Electron Microscopy

Bovine LDL receptor has been successfully incorporated into phospholipid vesicles using two different methods: (i) by simple detergent dialysis (Schneider, 1983) and (ii) as described here, by solubilization of preformed vesicles and detergent dialysis. Multilamellar liposomes are very easy to prepare but they are not suitable for structural studies of membrane proteins. On the other hand, small unilamellar vesicles suffer from the disadvantage that the surface of these vesicles has a high degree of curvature which affects many of the physical properties of the phospholipid in the vesicles. Therefore, for most studies of reconstituted receptors, it is important that the membrane protein is incorporated into large unilamellar vesicles (diameter >1000 Å) which most closely resemble biological membranes. Large unilamellar vesicles (LUVs) have been prepared using a variety of procedures, e.g. detergent dialysis, solvent evaporation, extrusion, etc. Schneider (1983) showed that the bovine LDL receptor could be reconstituted into EYPC bilayers using a detergent dialysis method. On the basis of gel filtration experiments, Schneider (1983) calculated the diameter of the receptor-containing vesicles to be in the range 2000−2700 Å. In the current study, the reconstituted EYPC vesicles containing the LDL receptor had diameters in the range 500−3000 Å as determined by electron microscopy, but with the majority in the range 2000−3000 Å. At a protein to lipid molar ratio of 1:10 000, and considering the surface area of phospholipid head group to be 70 $Å^2$ and bilayer thickness 40 Å, the expected number of receptor molecules per single bilayer vesicle is 20−80. Previous studies (Saxena & Shipley, 1992; Saxena, 1994) using negative-stain electron microscopy showed that LDL receptor-containing vesicles prepared by detergent dialysis do bind gold-labeled LDL; however, these studies showed that a high percentage of vesicles prepared by simple detergent dialysis contained more than one bilayer. A significant improvement in the production of unilamellar EYPC vesicles containing the LDL receptor has been achieved by using preformed vesicles made by extrusion, followed by the addition of detergent-solubilized receptor, and then dialysis to remove detergent. These reconstituted vesicles were almost exclusively unilamellar (diameter, 2000−3000 Å) and somewhat larger than the size of the original preformed vesicles. It is probable that at the concentration of the detergent used, a complete disruption of the bilayer of the vesicles occurs prior to reformation on

removal of the detergent. As shown in Figure 8, cryoelectron microscopy shows linear projections from the bilayer surface and suggests an extended structure (length approximately 120 Å) for the extracellular region (comprising Domains I, II, and III) of the LDL receptor.

Electron microscopy has become a very powerful technique for structure determination of membrane proteins reconstituted with lipids. Successful incorporation of the LDL receptor into large unilamellar vesicles has paved the way for detailed structural studies of the receptor and its interaction with its ligand, LDL. Our initial studies of the reconstituted vesicles using cryoelectron microscopy confirmed the unilamellar nature of the reconstituted vesicles and showed the receptor to be present in two orientations (i.e. on the outside and inside vesicle surfaces, see Figure 8). Since the extracellular domain forms the major portion (92%) of the receptor, it is straightforward to distinguish between the two orientations. Labeling studies with monoclonal antibodies directed against the N-terminus and the C-terminus of the receptor would clearly distinguish between the two orientations. Future studies will focus on (i) incorporating more copies of the LDL receptor into each vesicle, (ii) labeling of the reconstituted LDL receptor using LDL, LDL receptor antibodies, or their gold-labeled counterparts, and (iii) attempts to produce 2D crystals of the receptor. This approach should ultimately lead to a picture of the LDL receptor in a membrane environment and also provide a vehicle for studying structural aspects of the interaction of the LDL receptor with its ligand LDL.

ACKNOWLEDGMENT

We thank Drs. Joseph L. Goldstein and Michael S. Brown (University of Texas Southwestern Medical Center, Dallas, TX) for providing us with the monoclonal antibody IgG-4A4. Also, we acknowledge helpful advice from Robert A. Reed on the purification of the LDL receptor and from Drs. Donna Cabral-Lilly and Mary T. Walsh on electron microscopy and CD techniques, respectively. Technical assistance was provided by D. Gantz, A. Tercyak, C. England, M. Gigliotti, and C. Curry.

REFERENCES

Bansal, A., & Gierasch, L. M. (1991) *Cell 67*, 1195−1201.
Beisiegel, U., Schneider, W. J., Goldstein, J. L., Anderson, R. G., & Brown, M. S. (1981) *J. Biol. Chem. 256*, 11923−11931.
Beisiegel, U., Schneider, W. J., Brown, M. S., & Goldstein, J. L. (1982) *J. Biol. Chem. 257*, 13150−13156.
Bieri, S., Djordjevic, J. T., Daly, N. L., Smith, R., & Kroon, P. A. (1995) *Biochemistry 34*, 13059−13065.
Brown, M. S., & Goldstein, J. L. (1986) *Science 232*, 34−47.
Chang, C. T., Wu, C.-S. C., & Yang, J. T. (1978) *Analytical Biochemistry 91*, 13−31.
Chou, P. Y., & Fasman, G. D. (1974a) *Biochemistry 13*, 211−222.
Chou, P. Y., & Fasman, G. D. (1974b) *Biochemistry 13*, 222−245.
Cummings, R. D., Kornfeld, S., Schneider, W. J., Hobgood, K. K., Tolleshaug, H., Brown, M. S., & Goldstein, J. L. (1983) *J. Biol. Chem. 258*, 15261−15273.
Daly, N. L., Scanlon, M. J., Djordjevic, J. T., Kroon, P. A., & Smith, R. (1995a) *Proc. Natl. Acad. Sci. U.S.A. 34*, 14474−14481.
Daly, N. L., Djordjevic, J. T., Kroon, P. A., & Smith, R. (1995b) *Biochemistry 34*, 14474−14481.
De Loof, H., Rosseneu, M., Brasseur, R., & Ruysschaert, J. M. (1986) *Proc. Natl. Acad. Sci. U.S.A. 83*, 2295−2299.
Esser, V., Limbird, L. E., Brown, M. S., Goldstein, J. L., & Russell, D. W. (1988) *J. Biol. Chem. 263*, 13282−13290.
Fariselli, P., Compiani, M., & Casadio, R. (1993) *Eur. Biophys. J. 22*, 41−51.
Goldstein, J. L., & Brown, M. S. (1982) *Med. Clin. N. Am. 66*, 335−362.
Goldstein, J. L., & Brown, M. S. (1983) in *The Metabolic Basis of Inherited Disease* (Stanbury, J. B., Wyngaarden, J. B., Frederickson, D. S., Goldstein, J. L., and Brown, M. S., Eds.) pp 672−712, McGraw-Hill, New York.
Goldstein, J. L., Brown, M. S., Anderson, R. G. W., Russell, D. W., & Schneider, W. J. (1985) *Annu. Rev. Cell Biol. 1*, 1−39.
Jahnig, F. (1989) in *Prediction of Protein Structure and the Principles of Protein Conformation* (Fasman, G. D., Ed.) pp 707−717, Plenum Press, New York.
Laemmli, U. K. (1970) *Nature (London) 227*, 680−685.
Lindgren, F. T., Jensen, L. C., & Hatch, F. T. (1972) in *Blood Lipids and Lipoproteins: Quantitation, Composition and Metabolism* (Nelson, G. L., Ed.) Wiley Interscience, New York.
Madden, T. D., & Cullis, P. R. (1984) *J. Biol. Chem. 259*, 7655−7658.
Pittman, R. C., Carew, T. E., Attie, A. D., & Steinberg, D. (1982) *J. Biol. Chem. 257*, 7994−8000.
Saxena, K. (1994) Membrane Receptors: Low Density Lipoprotein Receptor and Glycosphingolipids. Ph.D. Thesis, Boston University, Boston, MA, 1994.
Saxena, K., & Shipley, G. G. (1992) *Biophys. J. 61*, A263.
Schneider, W. J. (1983) *J. Cell. Biochem. 23*, 95−106.
Schneider, W. J. (1989) *Biochim. Biophys. Acta 988*, 303−317.
Schneider, W. J., Basu, S. K., McPhaul, M. J., Goldstein, J. L., & Brown, M. S. (1979) *Proc. Natl. Acad. Sci. U.S.A. 76*, 5577−5581.
Schneider, W. J., Goldstein, J. L., & Brown, M. S. (1980) *J. Biol. Chem. 255*, 11442−11447.
Schneider, W. J., Beisiegel, U., Goldstein, J. L., & Brown, M. S. (1982) *J. Biol. Chem. 257*, 2664−2673.
Schneider, W. J., Goldstein, J. L., & Brown, M. S. (1985) *Methods Enzymol. 109*, 405−417.
Soutar, A. K. (1992) *J. Intern. Med. 231*, 633−641.
Tolleschaug, H., Goldstein, J. L., Schneider, W. J., & Brown, M. S. (1982) *Cell 30*, 715−724.
Yamamoto, T., Davis, C. G., Brown, M. S., Schneider, W. J., Casey, M. L., Goldstein, J. L., & Russell, D. W. (1984) *Cell 39*, 27−38.
Yokoyama, C., Wang, X., Briggs, M. R., Admon, A., Hua, X., Goldstein, J. L., & Brown, M. S. (1993) *Cell 75*, 187−197.

BI971579P